Supplement of Hydrol. Earth Syst. Sci., 30, 1755–1778, 2026
https://doi.org/10.5194/hess-30-1755-2026-supplement

Hydrology and Earth System Sciences
Open Access
EGU

Supplement of

Exploring groundwater-surface water interactions and recharge in fractured mountain systems: an integrated approach

Sofia Ortenzi et al.

Correspondence to: Lucio Di Matteo (lucio.dimatteo@unipg.it)

S1. Description of EO datasets

S1.1. Integrated Multi-satellitE Retrievals for Global Precipitation Measurements (GPM IMERG)

The GPM IMERG algorithm (Huffman et al., 2023). intercalibrates, merges, and interpolates precipitation estimates from GPM satellites, providing a half-hourly rainfall product (also available monthly and daily) with a spatial resolution of 0.1°x0.1° (about 10 km). The system is run three times, providing "Early," "Late," and "Final" rainfall estimates. The "Final" product is calibrated with monthly data from rain gauges and is released about four months after the observation month. Navarro et al. (2019) reported overall agreement of GPM IMERG data with the ENSEMBLES OBbservation (E-OBS) gridded dataset over Europe in the spatial distribution of mean precipitation ($R^2 = 0.8$), with discrepancies in mountainous regions along the Italian Peninsula.

S1.2 European Reanalysis 5th generation (ERA5-Land)

ERA5-Land (Muñoz Sabater, 2019; C3S, 2022) is a state-of-the-art land surface reanalysis dataset released by the European Centre for Medium-Range Weather Forecasts (ECMWF) within the Copernicus Climate Change Service (C3S). It provides globally high-resolution (about 9 km) estimates of land surface variables at multiple temporal resolutions, including precipitation at hourly resolution. As reported by Lavers et al. (2022), the standard deviation of the ERA5-minus-observed precipitation differences ranges between 2.5 and 10 mm/day in different seasons across Italy.

S1.3 The Meteorological Reanalysis Italian Dataset (MERIDA)

MERIDA (Bonanno et al., 2019) is a more regionally focused reanalysis product (resolution of about 7 km). It consists of dynamically downscaling the ERA5 global reanalysis fields using the Weather Research and Forecasting (WRF-ARW) mesoscale model (Skamarock et al., 2008). As reported in Bonanno et al. (2019), the robustness of MERIDA is guaranteed by the assimilation of the surface-based (SYNOP) data and the application of the Optimal Interpolation (OI) technique on the 2 m temperature and precipitation fields simulated by WRF. Sarigil et al. (2024) reported a correlation coefficient ($R > 0.60$) between ground-based and MERIDA observations across all regions of central and northern Italy.

S1.4 The Modified Conditional Merging (MCM) algorithm

The MCM algorithm (Pignone et al., 2015) generates precipitation estimates by blending data from this national rain-gauge and radar networks. After defining the spatiotemporal domain of interest, rainfall data from each rain gauge are interpolated using the GRISO method (random generator of spatial interpolation from uncertain observations; Pignone et al., 2010). The same procedure was performed on radar data. Precipitation data are sampled at rain gauge locations using radar data maps, and the same GRISO parameters are used to interpolate rain gauge data (e.g., Loglisci et al., 2024). Afterwards, precipitation data from the original radar map and from GRISO interpolation of the radar data are compared. Finally, the sum of the difference map and the rain gauge interpolation provides the MCM map.

S1.5 IT-SNOW product

Snow Water Equivalent (SWE) data were derived from the IT-SNOW product (Avanzi et al., 2023) developed by CIMA Research Foundation for the Italian Civil Protection Department. IT-SNOW is a snow reanalysis for Italy that blends modeling, in situ data, and satellite observations, with a spatial resolution of about 500 m. It is a snow reanalysis providing estimates of snow patterns in topographically and climatically complex regions across Italy (Avanzi et al., 2023). The dataset (IT-SNOW v4.0) includes daily reanalyzed outputs of Snow Water Equivalent (SWE), snow depth, density, and bulk liquid water content from S3M Italy for water years 2010 through 2024 (the dataset is freely available at https://zenodo.org/records/14093436). Avanzi et al. (2023) validated the SWE using IT-SNOW in three Italian regions, obtaining the following metrics: Pearson correlation coefficients between 0.45 and 0.81, RMSE between 95 mm and 290 mm, and bias between -112 mm and 82 mm.

S1.6 MOD16A2 v061 (MODIS)

The MOD16A2 v061 product provides 8-day, monthly, and annual datasets at a 500 m pixel size using a modified Penman-Monteith method from 2002 to the present (Mu et al., 2011). The evapotranspiration values from this remote sensing correspond to the sum of the evaporation from the wet canopy surface (E_{Wet}), the transpiration from the dry canopy surface (T_{Dry}), and the evaporation from the soil surface (E_{Soil}) (e.g., Gallego et al., 2023). As reported by Castelli (2021), the MODIS daily RMSE was below 1.5 mm/day, and the r coefficient ranged from 0.71 to 0.83.

S1.7 EUMETSAT LSA SAF (Land Surface Analysis Satellite Application Facility)

The EUMETSAT Land Surface Analysis Satellite Application Facility (LSA SAF) provides global estimates of net evapotranspiration derived from Meteosat Second Generation (MSG/SEVIRI) observations. The evapotranspiration product (DMETv3) is based on physically based surface energy balance approaches and is available at a daily temporal resolution on a regular 0.05° × 0.05° spatial grid (Trigo et al., 2011). For the validation of the EUMETSAT LSA SAF against reference evapotranspiration at different sites in Europe, see Trigo et al. (2011).

S1.8 Global Land Evaporation Amsterdam Model (GLEAM)

The GLEAM (version GLEAM4) model combines satellite observations, reanalysis data, and data assimilation techniques to represent the key processes controlling evapotranspiration. providing estimates of terrestrial evaporation and its individual components at the global scale. Net evapotranspiration is estimated at a daily temporal resolution and 0.1° spatial resolution (Miralles et al., 2025). As reported by Martens et al. (2017), despite regional differences, the quality of the evaporation fluxes using the previous version of GLEAM has an average correlations against eddy-covariance measurements ranging between 0.78 and 0.81 for the different data sets.

S1.9 ECO_L3T_JET (ECOSTRESS)

The ECOsystem Spaceborne Thermal Radiometer Experiment on Space Station (ECOSTRESS) mission provides high-resolution thermal infrared observations from the International Space Station (ISS) to investigate land surface temperature, plant water use, and vegetation stress. The ECOSTRESS Tiled Evapotranspiration Instantaneous and Daytime Level-3 product (ECO_L3T_JET) provides estimates of actual evapotranspiration

derived from surface energy balance modeling at ~70 m spatial resolution. The product is generated using a Priestley–Taylor–based framework driven by ECOSTRESS thermal infrared observations and ancillary meteorological and surface information. According to Fisher et al. (2020), ECOSTRESS LE matched well with site measurements (instantaneous: r^2 = 0.88; overall bias = 8%; normalized RMSE = 6%), showing good correlations and bias across a range of vegetation classes, climate zones, and times of day.

S2. ET by Thornthwaite-Mather method

The Thornthwaite-Mather (1955, 1957) method has been commonly used in mountain areas of Central Italy, and ET estimations have been found to be reliable (e.g., Di Matteo et al., 2017; Mammoliti et al., 2021; Rossi et al., 2022). This method was chosen because standard climatological records of solar radiation (sunshine), air temperature, humidity, and wind speed are either unavailable for the period of analysis or contain significant data gaps. As a result, more detailed methods such as the FAO-56 Penman–Monteith equation (Allen et al., 1998) could not be applied. The monthly ET values were computed over the hydrogeological year (from October to the following September) using the WaterbaLANce WebApp based on the Thornthwaite–Mather method developed by Mammoliti et al. (2021). Since the Ussita catchment is mainly characterized by leptosol (very shallow soils over hard rocks or calcareous materials; Costantini et al., 2012, https://esdac.jrc.ec.europa.eu/images/Eudasm/IT/2012Carta_Suoli_Italia.jpg) and is covered by about 90% of forests (based on the CORINE Land Cover 2018 database), the Available Water Capacity (AWC) was set to 100 mm and 150 mm (Thornthwaite-Mather, 1957).

S3. BIGBANG dataset

The BIGBANG 8.0 dataset "Nationwide GIS-Based hydrological budget on a regular grid" presents WS values, computed from ground-based data and ET using the Thornthwaite-Mather method over a 1x1 km grid. The dataset is available for download from the SINAnet ISPRA website (Sistema Informativo Nazionale Ambiente of Istituto Superiore per la Protezione e Ricerca Ambientale; https://groupware.sinanet.isprambiente.it/bigbang-data/library/bigbang_80/ascii_grid).

S4. Acquisition and treatment of hydrochemical and isotopic data

In the field, pH, temperature, and electrical conductivity were determined by using a multi-parameter portable meter (model XS PC 7 Vio), whilst the HCO_3^- concentration was determined by acidimetric titration in a sample of 250 ml, adding HCl 0.1 N with a portable dosimeter and using methyl orange as a colorimetric indicator (e.g., Donnini et al., 2016; Frondini et al., 2019; Chiodini et al., 2021; Donnini et al., 2025). The wide-mouthed funnel collects a representative rainfall sample, while the narrow nozzle directs the rainwater into a collection bottle, thereby reducing the water's surface area exposed to the atmosphere and minimizing evaporation. To collect precipitation in the form of snow, a dark tube was placed above the funnel of the PR3 station (elevation of about 1200 m a.s.l., Fig. S1). This tube allowed the snow to be collected and melted before it entered in the collection bottle. The concentration of major soluble cations and anions of stream water (Ca^{2+}, Mg^{2+}, Na^+, K^+, SO_4^{2+}, Cl^-) was obtained by suppressed ionic chromatography (AQUION and ICS-2100 Dionex supplied by ThermoFisher Scientific, Waltham, MA, USA). Multi-ion calibration standards were prepared from single-component standard solutions for ion chromatography (Fluka-TraceCERTTM, 1000 ± 4 ppm, Honeywell International Inc., Charlotte,

NC, USA). The isotopic analyses were performed through standard mass spectrometry (PICARRO L2130-I Cavity Ring-Down Spectroscopy CRDS). The linearity of the calibration curves was verified over the 0.5-50 ppm range. The values of δD ($^{2}H/^{1}H$) and of $\delta^{18}O$ ($^{18}O/^{16}O$) are referred to as δ (‰) of the standard V-SMOW (Vienna Standard Mean Ocean Water). Analytical errors are: ±1‰ for δD, ±0.08‰ for $\delta^{18}O$.

S5. Supplementary tables and figures

Table S1: Characteristics of ground-based thermo-pluviometric and snow depth gauges.

Name	ID	Altitude (m a.s.l.)	Type	Managing authority	Observation period
ENDESA	RT-2695	700	Pluviometer	SIRMIP	from Dec-2006
Ponte Tavola	RT-2698	709	Pluviometer	SIRMIP	from Dec-2006
Ussita	RT-1651	749	Pluviometer	SIRMIP	from Nov-2003
	RT-1653		Thermometer		
Gualdo	RT-3150	1000	Pluviometer	SIRMIP	from Jul-2017
	RT-3152		Thermometer		
Casali	-	1090	Pluviometer	CNR-IRPI	from Jun-2022
			Thermometer		
Pizzo Tre Vescovi	RT-1787	1825	Thermometer	SIRMIP	from Aug-2002
	RT-1788		Snow depth		
Monte Bove Sud	RT-1851	1853	Pluviometer	SIRMIP	from Aug-2002
	RT-1853		Thermometer		from Aug-2002
	RT-1854		Snow depth		from Nov-2007
Casali	PR1	1071	Rain collector	CNR-IRPI	from Nov-2023
Ussita	PR2	770			
Val di Panico	PR3	1237			
Sorbo	PR4	983			

Table S2: Limit of Detection (LOD) and Limit of Quantitation (LOQ) values for cations.

Analyte	Na^{+}	K^{+}	Mg^{2+}	Ca^{2+}
LOD (mg/L)	0.4	0.3	0.4	0.9
LOQ (mg/L)	1.3	1.2	1.3	2.9

Table S3: Limit of Detection (LOD) and Limit of Quantitation (LOQ) values for anions.

Analyte	Cl^{-}	SO_4^{-2}
LOD (mg/L)	0.8	1.0
LOQ (mg/L)	2.7	3.3

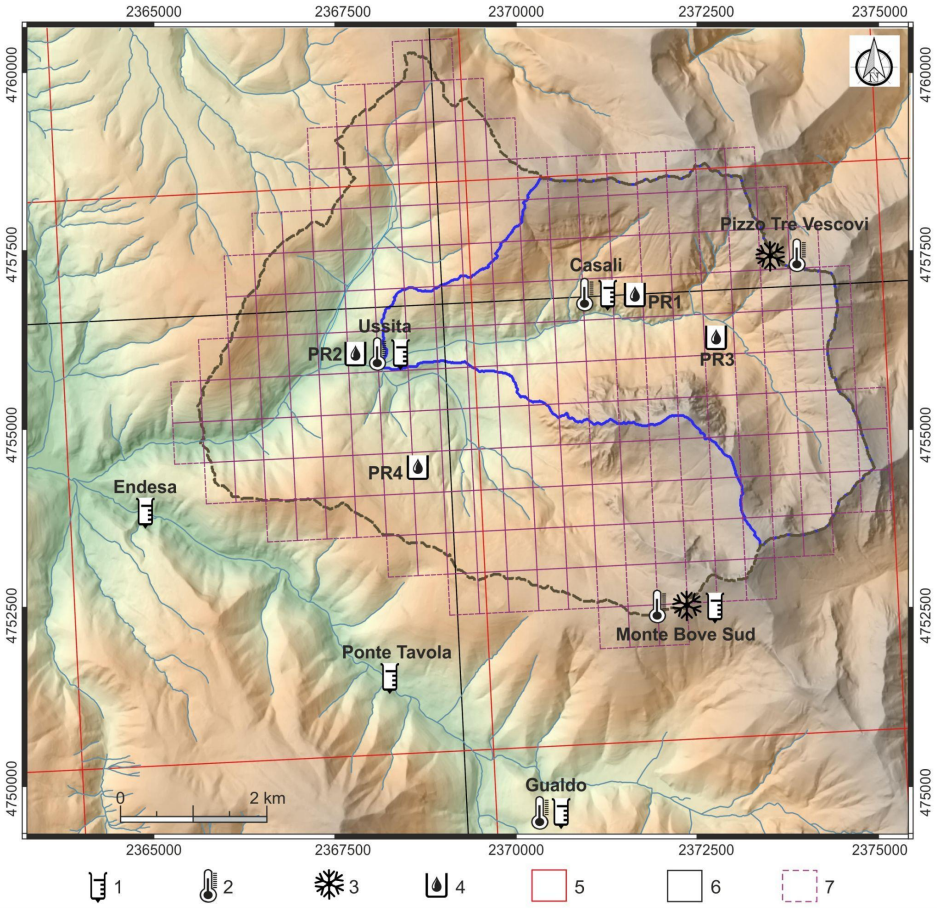

Figure S1: The location of thermo-pluviometric and snow depth gauges with rain water samples for isotopic analyses and dataset product grids. 1 – rainfall; 2 – air temperature; 3 – snow depth; 4 – isotopic rain collectors; 5 – MERIDA grid; 6 – ERA5-Land and IMERG grid; 7 – IT-SNOW grid.

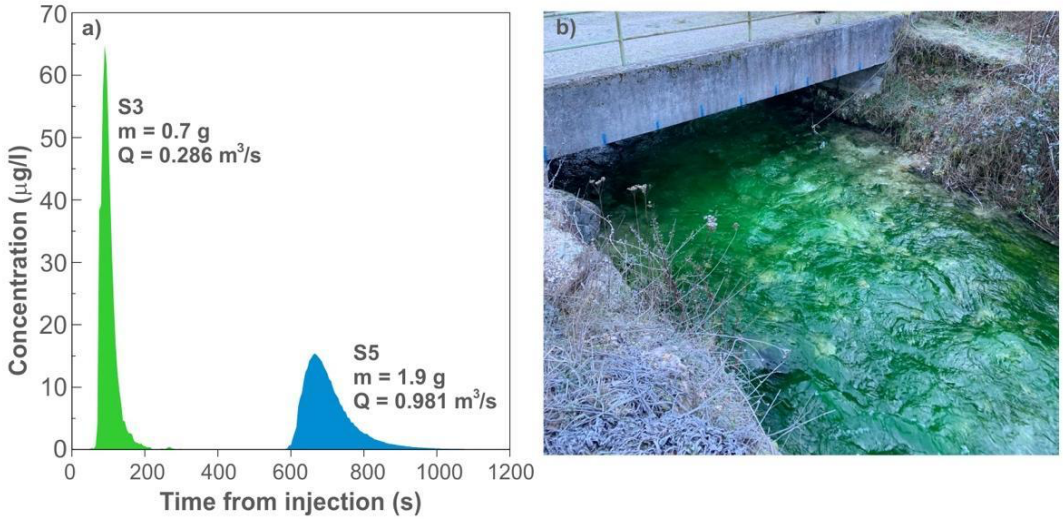

Figure S2: BTCs for S3 and S5 monitoring points on January 29, 2024, with details of: a) injected mass, and computed discharge; b) Na-Fluorescein passage in the monitoring point S5 during the test (b).

Table S4: Physical parameters (T: temperature, pH, EC: electrical conductivity) and major soluble ions of stream waters sampled in the Ussita catchment

ID	Date	T [°C]	pH	EC [µS/cm]	Ca^{2+} [mg/L]	Mg^{2+} [mg/L]	Na^{+} [mg/L]	K^{+} [mg/L]	HCO_3^{-} [mg/L]	SO_4^{2-} [mg/L]	Cl^{-} [mg/L]
S1	23/11/2023	6.60	8.33	216.00	42.71	0.20	1.08	0.34	129.32	1.55	1.96
S1	19/01/2024		8.48		43.68	0.20	1.21	0.34	144.69	2.49	2.26
S1	19/03/2024	8.10	8.04		43.85	0.20	1.11	0.34	135.66	2.29	2.18
S1	09/05/2024	6.30	8.68	190.00	42.69	0.20	1.06	0.34	137.05	2.24	2.11
S1	10/07/2024	5.60	7.99	158.80	43.21	0.20	1.05	0.34	142.01	1.84	1.70
S2	23/11/2023	8.10	8.08	237.00	47.33	0.96	1.93	0.03	146.64	3.37	0.11
S2	19/03/2024	9.80	8.53	188.50	46.79	0.88	1.64	0.01	142.98	2.86	0.08
S3	19/01/2024	7.90	8.57	226.00	45.03	0.86	2.12	0.34	163.97	2.55	2.73
S3	19/03/2024	9.00	8.70	268.00	46.98	0.88	1.92	0.34	152.26	2.94	3.05
S3	09/05/2024	8.30	8.83	201.00	45.18	0.80	1.82	0.34	157.69	2.74	2.62
S3	10/07/2024	13.40	8.78	199.00	45.08	0.93	1.95	0.34	159.58	2.82	2.83
I1	09/05/2024	9.30	8.18	264.00	58.29	2.54	2.42	0.34	165.11	6.92	7.44
I2	01/02/2024	8.20	8.44	299.00	47.10	8.39	2.10	0.70	166.90	17.88	3.77
I2	19/03/2024	11.30	7.81	405.00	47.67	8.97	7.97	0.77	176.17	18.88	12.55
I2	09/05/2024	8.80	8.27	274.00	47.25	8.46	2.12	0.34	189.10	16.94	3.76
I2	10/07/2024	10.80	7.97	353.00	46.78	8.61	2.15	2.94	176.90	17.57	5.77
S5	23/11/2023	9.70	7.79	302.00	52.73	5.95	2.04	0.34	161.77	20.20	4.24
S5	19/01/2024	9.80	8.33	302.00	52.15	6.10	2.36	0.34	178.85	20.78	4.68
S5	19/03/2024	9.60	8.20	316.00	50.79	5.16	2.03	0.34	164.94	15.91	4.13
S5	09/05/2024	10.00	8.44	271.00	49.40	5.53	1.90	1.18	170.80	19.10	4.47
S5	10/07/2024	13.20	8.40	277.00	52.59	6.34	2.25	1.39	183.98	21.42	5.09

Table S5: Isotopic composition of δD and $\delta^{18}O$ in stream and precipitation waters sampled within the Ussita catchment. For stream waters are also shown lc-excess values (na: not applicable).

ID	Date	Type	δD	$\delta^{18}O$	lc-excess
PR1	29/06/2023	Pluvio	-47.67	-8.21	na
PR1	21/07/2023	Pluvio	-30.48	-6.04	na
PR1	11/08/2023	Pluvio	-23.12	-5.73	na
PR1	22/09/2023	Pluvio	-30.7	-6.2	na
PR1	20/10/2023	Pluvio	-41.57	-7.44	na
PR1	02/11/2023	Pluvio	-35.68	-6.93	na

PR1	17/11/2023	Pluvio	-42.35	-8.12	na
PR1	07/12/2023	Pluvio	-79.4	-11.49	na
PR1	19/01/2024	Pluvio	-65.37	-10.06	na
PR1	19/03/2024	Pluvio	-55.85	-8.79	na
PR2	29/06/2023	Pluvio	-43.73	-7.6	na
PR2	21/07/2023	Pluvio	-28.89	-5.99	na
PR2	11/08/2023	Pluvio	-20.25	-5.08	na
PR2	22/09/2023	Pluvio	-26.07	-5.32	na
PR2	20/10/2023	Pluvio	-32.59	-6.42	na
PR2	02/11/2023	Pluvio	-31.51	-6.16	na
PR2	17/11/2023	Pluvio	-41.09	-7.49	na
PR2	07/12/2023	Pluvio	-63.37	-9.83	na
PR2	19/01/2024	Pluvio	-54.59	-8.84	na
PR2	19/03/2024	Pluvio	-47.17	-7.42	na
PR3	29/06/2023	Pluvio	-34.64	-6.04	na
PR3	21/07/2023	Pluvio	-23.23	-3.83	na
PR3	22/09/2023	Pluvio	-36.57	-7.43	na
PR3	20/10/2023	Pluvio	-49.51	-8.96	na
PR3	02/11/2023	Pluvio	-34.69	-6.41	na
PR3	17/11/2023	Pluvio	-49.03	-8.95	na
PR3	07/12/2023	Pluvio	-81.56	-12.14	na
PR3	19/01/2024	Pluvio	-75.1	-11.4	na
PR3	19/03/2024	Pluvio	-63.56	-10.17	na
PR4	29/06/2023	Pluvio	-47.06	-7.81	na
PR4	21/07/2023	Pluvio	-28.95	-6	na
PR4	11/08/2023	Pluvio	-18.81	-4.91	na
PR4	20/10/2023	Pluvio	-25.41	-5.53	na
PR4	02/11/2023	Pluvio	-15.34	-2.76	na
PR4	17/11/2023	Pluvio	-41.89	-7.77	na
PR4	07/12/2023	Pluvio	-65.39	-10.52	na
PR4	19/01/2024	Pluvio	-60.44	-9.67	na
PR4	19/03/2024	Pluvio	-56.51	-8.83	na
S2	29/06/2023	Stream	-70.06	-11.17	3.30

S2	21/07/2023	Stream	-67.57	-10.7	2.03
S2	11/08/2023	Stream	-69.1	-11.27	5.06
S2	22/09/2023	Stream	-68.28	-11.29	6.04
S2	20/10/2023	Stream	-65.77	-10.7	3.83
S2	02/11/2023	Stream	-69.58	-11.04	2.74
S2	17/11/2023	Stream	-68.25	-10.96	3.43
S2	07/12/2023	Stream	-68.52	-10.79	1.80
S2	19/01/2024	Stream	-67.85	-10.89	3.27
S2	19/03/2024	Stream	-67.66	-10.79	2.66
S3	19/01/2024	Stream	-68.26	-10.65	0.94
S3	19/03/2024	Stream	-67.35	-10.74	2.57
I2	01/02/2024	Stream	-70.24	-10.98	1.60
I2	19/03/2024	Stream	-68.07	-10.56	0.41
S5	29/06/2023	Stream	-70.35	-11.16	2.93
S5	21/07/2023	Stream	-68.09	-10.65	1.11
S5	11/08/2023	Stream	-68.58	-11.04	3.74
S5	22/09/2023	Stream	-67.65	-11.07	4.91
S5	20/10/2023	Stream	-66.08	-10.63	2.96
S5	02/11/2023	Stream	-69.4	-10.85	1.40
S5	17/11/2023	Stream	-67.01	-10.51	1.07
S5	07/12/2023	Stream	-69.34	-10.97	2.42
S5	19/01/2024	Stream	-67.33	-10.8	3.07

Table S6: Average (avg) and coefficient of variation (cv) for the physical parameters (T: temperature, pH, EC: electrical conductivity) and for major soluble ions (Ca^{2+}, Mg^{2+}, Na^{+}, K^{+}, HCO_3^{-}, SO_4^{2-}, and Cl^{-}) of Ussita stream waters.

ID	S1	S2	S3	I1	I2	S5
Samples	5	2	4	1	4	5
T_avg [°C]	6.65	8.95	9.65	9.30	9.78	10.46
T_cv [%]	16	13	26	na	15	15
pH_avg	8.30	8.31	8.72	8.18	8.12	8.23
pH_cv [%]	4	4	1	na	4	3
EC_avg [µS/cm]	188.27	212.75	223.50	264.00	332.75	293.60
EC_cv [%]	15	16	14	na	18	6
Ca_avg [mg/L]	43.23	47.06	45.57	58.29	47.20	51.53

Ca_cv [%]	1	1	2	na	1	3
Mg_avg [mg/L]	0.20	0.92	0.87	2.54	8.61	5.82
Mg_cv [%]	0	6	6	na	3	8
Na_avg [mg/L]	1.10	1.79	1.95	2.42	3.59	2.12
Na_cv [%]	6	11	6	na	82	9
K_avg [mg/L]	0.34	0.02	0.34	0.34	1.19	0.72
K_cv [%]	0	71	0	na	100	73
HCO_3_avg [mg/L]	137.75	144.81	158.38	165.11	177.27	172.07
HCO_3_cv [%]	4	2	3	na	5	5
SO_4_avg [mg/L]	2.08	3.12	2.76	6.92	17.82	17.82
SO_4_cv [%]	18	12	6	na	5	11
Cl_avg [mg/L]	2.04	0.10	2.81	7.44	6.46	4.52
Cl_cv [%]	11	22	7	na	64	8

Table S7: Average (avg) and coefficient of variation (cv) for δD, $\delta^{18}O$, and lc-excess (lc) of Ussita stream and precipitation waters. na: not applicable

ID	PR1	PR2	PR3	PR4	S2	S3	I2	S5
Samples	10	10	9	9	10	2	2	9
δD_avg [mg/L]	-45.22	-38.93	-49.77	-39.98	-68.26	-67.81	-69.16	-68.20
δD_cv [%]	38	35	40	47	2	1	2	2
δ18O_avg [mg/L]	-7.90	-7.02	-8.37	-7.09	-10.96	-10.70	-10.77	-10.85
δ18O_cv [%]	23	22	32	35	2	1	3	2
lc_avg [mg/L]	na	na	na	na	3.42	1.76	1.01	2.62
lc_cv [%]	na	na	na	na	38	66	84	49

Additional References

Allen, R. G., Pereira, L. S., Raes, D. and Smith, M.: FAO Irrigation and drainage paper No. 56, Rome: food and agriculture organization of the United Nations, 56(97), e156, ISBN 92-5-104219-5, 1998. Castelli, M.: Evapotranspiration changes over the European Alps: Consistency of trends and their drivers between the MOD16 and SSEBop algorithms. Remote Sensing, 13(21), 4316, doi:10.3390/rs13214316, 2021.

Chiodini, G., Caliro, S., Avino, R., Bini, G., Giudicepietro, F., De Cesare, W., Ricciolino, P., Aiuppa, A., Cardellini, C., Petrillo, Z., Selva, J., Siniscalchi, A. and Tripaldi, S.: Hydrothermal pressure-temperature control on CO2 emissions and seismicity at Campi Flegrei (Italy), J. Volcanol. Geotherm. Res., 414, 107245, doi:10.1016/j.jvolgeores.2021.107245, 2021.

Costantini, E. A. C., G. L'Abate, R. Barbetti, M. Fantappié, R. Lorenzetti, S. Magini: Soil Map of Italy, Consiglio per ricerca e la sperimentazione in agricoltura, Ministero delle Politiche Agricole Alimentari e Forestali, https://esdac.jrc.ec.europa.eu/images/Eudasm/IT/2012Carta_Suoli_Italia.jpg, 2012 (Accessed on 06-05-2025).

Donnini, M., Frondini, F., Probst, J. L., Probst, A., Cardellini, C., Marchesini, I. and Guzzetti, F.: Chemical weathering and consumption of atmospheric carbon dioxide in the Alpine region, Glob. planet. change, 136, 65-81, doi:10.1016/j.gloplacha.2015.10.017, 2016.

Donnini, M., Benigni, A., Dionigi, M., Massari, C., Cappelletti, D., Selvaggi, R., Fastelli, M., Scricciolo, E., Cencetti, C. and Marchesini, I.: Hydrology and atmospheric CO2 consumption by chemical weathering in a Mediterranean watershed, Catena, 252, 108868, doi:10.1016/j.catena.2025.108868, 2025.

Fisher, J. B., Lee, B., Purdy, A. J., Halverson, G. H., Dohlen, M. B., Cawse-Nicholson, K., Wang, A., Anderson, R.G., Aragon, B., Arain, M.A., Baldocchi, D.D., Baker, J.M., Barral, H., Bernacchi, C.J., Bernhofer, C., Biraud, S.C., Bohrer, G., Brunsell, N., Cappelaere, B., Castro-Contreras, S., Chun, J., Conrad, B.J., Cremonese, E., Demarty, J., Desai, A.R., De Ligne, A., Foltýnová, L., Goulden, M.L., Griffis, T.J., Grünwald, T., Johnson, M.S., Kang, M., Kelbe, D., Kowalska, N., Lim, Jong-Hwan, Maïnassara, I., McCabe, M.F., Missik, J.E.C., Mohanty, B.P., Moore, C.E., Morillas, L., Morrison, R., Munger, J.W., Posse, G., Richardson, A.D., Russell, E.S., Ryu, Y., Sanchez-Azofeifa, A., Schmidt, M., Schwartz, E., Sharp, I., Šigut, L., Tang, Y., Hulley, G., Anderson, M., Hain, C., French, A., Wood, E. and Hook, S.: ECOSTRESS: NASA's next generation mission to measure evapotranspiration from the international space station, Water Resources Research, 56(4), e2019WR026058, doi:10.1029/2019WR026058, 2020.

Frondini, F., Cardellini, C., Caliro, S., Beddini, G., Rosiello, A. and Chiodini, G.: Measuring and interpreting CO2 fluxes at regional scale: the case of the Apennines, Italy, J. Geol. Soc., 176(2), 408-416, doi:10.1144/jgs2017-169, 2019.

Skamarock, W. C., Klemp, J. B., Dudhia, J., Gill, D. O., Barker, D. M., Duda, M. G., Huang, X.-Y., Wang, W. and Powers, J. G.: A description of the advanced research WRF Version 3, NCAR tech. note ncar/tn-475+str, doi:10.5065/D68S4MVH, 2008.

Lavers, D. A., Simmons, A., Vamborg, F. and Rodwell, M. J.: An evaluation of ERA5 precipitation for climate monitoring, Quarterly Journal of the Royal Meteorological Society, 148(748), 3152-3165, doi:10.1002/qj.4351, 2022.

Loglisci, N., Boni, G., Cauteruccio, A., Faccini, F., Milelli, M., Paliaga, G. and Parodi, A.: The role of citizen science in assessing the spatiotemporal pattern of rainfall events in urban areas: a case study in the city of Genoa, Italy, NHESS, 24(7), 2495-2510, doi:10.5194/nhess-24-2495-2024, 2024.

Mammoliti, E., Fronzi, D., Mancini, A., Valigi, D. and Tazioli, A.: WaterbalANce, a WebApp for Thornthwaite–Mather Water Balance Computation: comparison of applications in two European watersheds, Hydrology, 8(1), 34, doi:10.3390/hydrology8010034, 2021.

Martens, B., Miralles, D. G., Lievens, H., Van Der Schalie, R., De Jeu, R. A., Fernández-Prieto, D., Beck H.E., Dorigo W.A. and Verhoest, N. E.: GLEAM v3: Satellite-based land evaporation and root-zone soil moisture, Geoscientific Model Development, 10(5), 1903-1925, doi:10.5194/gmd-10-1903-2017, 2017.

Rossi, M., Donnini, M., and Beddini, G.: Nationwide groundwater recharge evaluation for a sustainable water withdrawal over Italy, J. Hydrol. Reg. Stud., 43, 101172, doi:10.1016/j.ejrh.2022.101172, 2022.

Sarigil, G., Neri, M. and Toth, E.: Evaluation of national and international gridded meteorological products for rainfall-runoff modelling in Northern Italy, Journal of Hydrology: Regional Studies, 56, 102031, doi:10.1016/j.ejrh.2024.102031, 2024.